

Direct-Sequence Spread-Spectrum Acquisition for High Dynamic Environments via Signal Partitioning

Derrick A. Chu, *Student Member, IEEE*, John R. Barry, *Senior Member, IEEE*

Abstract—Time-varying Doppler shifts can arise in low-earth orbit satellites and other high-dynamic environments, and are a significant impediment to the acquisition of spread-spectrum signals. In this paper we propose delay-Doppler efficient exhaustive search (DEES), an efficient algorithm that can acquire direct-sequence spread-spectrum signals with long spreading codes in the presence of both Doppler rate and Doppler frequency shifts. DEES combines the second-order keystone transform and the fractional Fourier transform to mitigate the effects of time-varying channel delays, before jointly estimating both the code phase offset and the Doppler frequency. Numerical results demonstrate that DEES can acquire spread-spectrum signals in the high-acceleration regime of the low-earth orbit satellite channel at low SNR.

Index Terms—Satellite communications, low-earth orbit (LEO), Spread-spectrum acquisition, keystone transform, Fractional Fourier transform (FrFT), Doppler rate.

I. INTRODUCTION

Low-earth orbit (LEO) satellite channels present several challenges to reliable communication, notably time-varying delays, large Doppler frequency shifts, and high Doppler rates, especially at high carrier frequencies [1]–[3]. These so-called high dynamic environments are not limited to LEO satellite communications, and have been reported in both hypersonic vehicle and space communications [4]–[6]. For direct-sequence spread-spectrum (DSSS) communications, which are frequently used in military applications due to their favorable low probability of intercept (LPI) and anti-jam characteristics [7], large Doppler variations can prevent proper spreading code acquisition, particularly when the spreading code is long [8].

There are many existing DSSS acquisition techniques that can be utilized when the received code phase offset is approximately static, and the Doppler frequency is constant [9]–[15], or when the code phase varies linearly with time [16]–[18]. There are fewer techniques that can acquire a DSSS signal when the Doppler rate is non-negligible [19]–[21]. [19], [20] proposes an algorithm based on the fractional Fourier transform (FrFT) to estimate and compensate for Doppler rate in DSSS signals. [21] uses a convex optimization algorithm to estimate the code phase and Doppler frequency.

There have been several techniques pioneered in the field of radar signal processing that can estimate and compensate for target acceleration (proportional to Doppler rate), before jointly estimating the range and velocity [22]–[25]. However, these techniques are developed under the assumption that the transmitted signal is a linear frequency modulated (LFM)

chirp, and many use specific properties of LFM signals which makes them unsuitable for DSSS acquisition.

We propose delay-Doppler efficient exhaustive search (DEES), an algorithm that can efficiently acquire a DSSS signal in the face of large Doppler shifts and high Doppler rate. We first derive DEES as an approximation of the optimal exhaustive search in the simplified case of a static code phase offset, then augment DEES with second-order keystone transforms and the fractional Fourier transform to allow it to handle time-varying code phases and time-varying Doppler frequency shifts. Finally, we characterize the acquisition performance of DEES for long code DSSS signals in the high-acceleration regime of the LEO satellite channel.

II. PROBLEM STATEMENT

Given the vast existing literature on DSSS acquisition for static code phase offsets and constant Doppler [7], [9]–[14], [16], we specifically focus on the time-varying Doppler aspect of the problem, and ignore non-essential features such as data modulation which have been discussed in [14]. We cast acquisition as a two stage process: the first stage is the parameter estimation stage in which the receiver must estimate the time-varying code phase offset. The second stage is the detection stage in which the receiver must determine, based on the estimated parameters, if the locally generated spreading code is sufficiently aligned with the received signal such that acquisition has been achieved, and the receiver can then proceed to the tracking phase [26].

We model the baseband IQ samples at the receiver as:

$$r_k = \alpha x_{k-d_k} e^{-j\omega_0 d_k} + n_k, \quad (1)$$

where α is an unknown complex channel gain, $\omega_0 = 2\pi f_c T_c$ is the normalized radian carrier frequency, f_c is the carrier frequency in Hz, T_c is the chip period, $f_s = 1/T_c$ is the sampling frequency, and the components of the noise vector n_k are *i.i.d.* $\mathcal{CN}(0, 2\sigma^2)$. The transmitted binary DSSS signal x_k is assumed to be known to the receiver, and is non-zero only for $k \in \{0, 1, \dots, L-1\}$. To account for the case when the delay d_k in (1) is not an integer, we define $x_{k-d} = \sum_n x_n \text{sinc}((k-n)-d)$; for readability this interpolating sinc is suppressed.

To reflect the presence of both Doppler rate and Doppler frequency shift, we adopt a quadratic model for the code phase offset, which is modeled as a time-varying delay d_k , namely:

$$d_k = d_0 - b_0 k - b_1 k^2, \quad (2)$$

where d_0 is the initial code phase offset in chips, $b_0 = f_{D,0}/f_c$ is a constant proportional to the initial Doppler frequency $f_{D,0}$ in Hz, and $b_1 = f_A T_c / (2f_c)$ is a constant proportional to the Doppler rate f_A in Hz/s, which is assumed to be constant.

The receiver is assumed to have knowledge of the maximum values of the coefficients in (2), i.e. $|d_0| \leq |d_{0,\max}|$, $|b_0| \leq |b_{0,\max}|$, and $|b_1| \leq |b_{1,\max}|$. Furthermore, implicit in (1) is the assumption that the maximum possible Doppler frequency shift is just a small fraction of the chip rate, that is $|b_{0,\max} + Lb_{1,\max}/2|f_c T_c << 1$.

This paper solves the following problem: Given knowledge of the received signal model in (1) and the quadratic delay model in (2), estimate the parameters $\{d_0, b_0, b_1\}$ that maximize the acquisition statistic [26], [27]:

$$z = \left| \sum_{k=-\infty}^{\infty} r_k x_{k-\hat{d}_k}^* e^{+j\omega_0 \hat{d}_k} \right|^2, \quad (3)$$

where \hat{d}_k is the estimate of d_k .

III. STATIC CODE PHASES

In this section we restrict our attention to the simpler case of zero Doppler rate ($b_1 = 0$), static code phase offsets ($x_{k-d_k} = x_{k-d_0}$), and $\alpha = 1$. For this static case, we will derive the “core form” of DEES from the optimal exhaustive search [28]. Later, in Section IV, we consider the full model in (1) and augment DEES to handle a time-varying code phase offset and time-varying Doppler.

When the Doppler rate is zero, the normalized radian Doppler frequency $\omega_D = 2\pi f_c T_c b_0$ is constant, and the code phase offset can be treated as static when $|Lb_0| << 1/2$. In this case, only d_0 and b_0 need to be estimated. The maximum-likelihood (ML) estimates for ω_D and d_0 can be found from an exhaustive search over all possible candidate code phases and Doppler frequencies, where for each candidate Doppler frequency ω and code phase d the received signal r_k is multiplied by $e^{-j\omega k}$, then correlated with the delayed spreading code x_{k-d} . This is equivalent to the nested optimization:

$$\hat{\omega}_D = \arg \max_{\omega} \max_d \operatorname{Re} \left\{ \sum_k e^{-j\omega k} r_k x_{k-d}^* \right\}, \quad (4)$$

where $\operatorname{Re}\{ \cdot \}$ takes the real part of its argument. The inner optimization of (4) can be efficiently implemented using a matched filter (MF). In particular, the integer value of d that maximizes the inner sum can be found by passing $e^{-j\omega k} r_k$ through a filter matched to x_k , producing the output

$$\tilde{y}_k = e^{-j\omega k} r_k * x_{-k}^*, \quad (5)$$

and choosing d as the time at which the real part of the MF output achieves its maximum value.

Since x_k is of length L , we can select an integer N that divides L evenly, and partition the length L signal into N segments, each of length L/N . In particular, let us define the n th segment, for $n \in \{0, 1, \dots, N-1\}$, by

$$x_k^{(n)} = x_{k+nL/N} w_k, \quad (6)$$

where w_k is the rectangular window $w_k = 1$ for $k \in \{0, 1, \dots, L/N-1\}$, and $w_k = 0$ for other k . According to this definition, all segments are non-zero only for k in this same interval. The MF output of (5) can be written in terms of these segments as:

$$\begin{aligned} \tilde{y}_k &= e^{-j\omega k} r_k * \sum_{n=0}^{N-1} x_{-k-nL/N}^{(n)*} \\ &= \sum_{n=0}^{N-1} e^{-j\omega(k+nL/N)} r_{nL/N+k} * x_{-k}^{(n)*}. \end{aligned} \quad (7)$$

The last line of (7) describes a parallel implementation of the length L MF, in which the MF output is computed by adding the outputs of a bank of N matched filters, each of length L/N , one for each signal segment.

Since d is restricted to $\mathcal{D} = \{-d_{\max}, \dots, 0, \dots, d_{\max}\}$ where d_{\max} is the maximum value of $|d_k|$, \tilde{y}_k need only be evaluated for $k \in \mathcal{D}$. When k is restricted in this manner, we can replace the input $e^{-j\omega(k+nL/N)} r_{nL/N+k}$ to the n th segment MF by a windowed version that explicitly discards the irrelevant portions of the received signal, namely:

$$\tilde{r}_k^{(n)} = e^{-j\omega(k+nL/N)} r_{nL/N+k} w'_k, \quad (8)$$

where w'_k is a unit-height rectangular window that is non-zero only in the interval $k \in \mathcal{I}' = \{-d_{\max}, \dots, L/N + d_{\max} - 1\}$.

A key step in our derivation is to recognize that, when the window w'_k in (8) is sufficiently short, or equivalently when the candidate normalized Doppler ω is sufficiently small relative to the window length $L/N + 2d_{\max}$, the phase factor $e^{-j\omega k}$ in (8) will be approximately constant over the duration of the window, taking the same value throughout the duration of the window that it takes at time $k = 0$. We denote this as the constant-phase-approximation (CPA). Under CPA, we can approximate the factor $e^{-j\omega k}$ by 1 in (8), so that the input to the n th MF can be written as:

$$\tilde{r}_k^{(n)} \approx e^{-j\omega nL/N} r_{nL/N+k} w'_k. \quad (9)$$

Unlike (8), the complex exponential in (9) is a constant that can be moved to the output of the MF. Therefore, instead of feeding $\tilde{r}_k^{(n)}$ as the input to the n th MF, we can instead feed the following signal:

$$r_k^{(n)} = r_{nL/N+k} w'_k, \quad (10)$$

and then multiply the output of the n th MF by the constant $e^{-j\omega nL/N}$ before adding.

Let $y_k^{(n)}$ denote the output of the n th MF at time k , when the uncompensated segment $r_k^{(n)}$ from (10) is its input. Then we can approximate the output of the overall MF in (7) by multiplying each segment MF output by the appropriate constant before adding, yielding

$$y_k = \sum_{n=0}^{N-1} e^{-j\omega nL/N} y_k^{(n)}. \quad (11)$$

For k fixed, this can be viewed as a sampled DTFT of the MF bank outputs $y_k^{(n)}$, viewed as a function of n . For

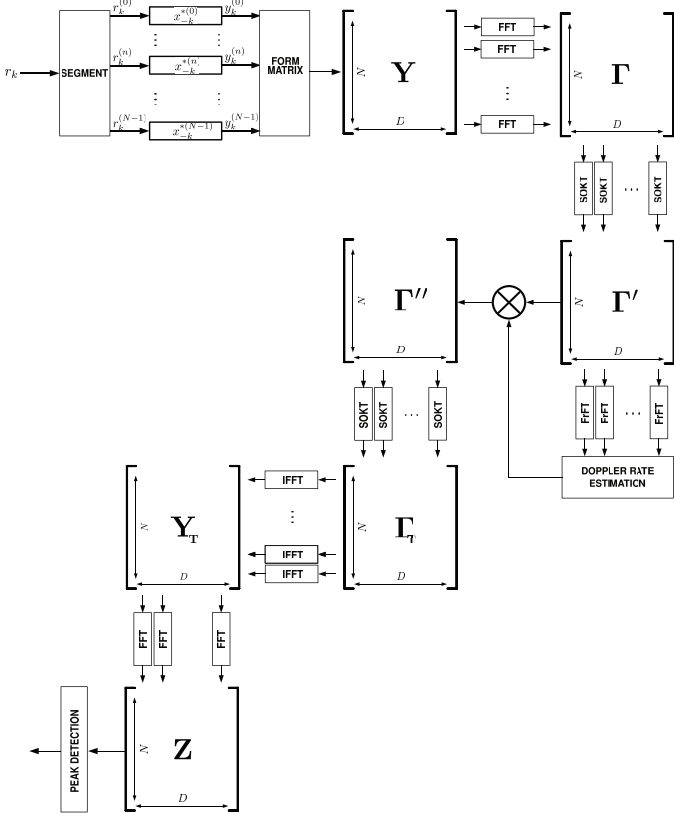


Fig. 1: Block diagram of the delay-Doppler efficient exhaustive search (DEES) algorithm.

the special case when the set of candidate frequencies ω is restricted to be of the form $\omega = 2\pi m/L$ for $m \in \mathcal{M} = \{0, \pm 1, \dots, \pm(N/2 - 1)\}$, then (11) is equivalent to the DFT, which can be efficiently implemented with the FFT.

We now summarize this proposed algorithm, which we will refer to as core DEES. The received sequence r_k is partitioned into N segments, and each segment $r_k^{(n)}$ is passed through a filter matched to that segment of the spreading code, with impulse response $x_{-k}^{*(n)}$. The MF outputs are then collected into a $N \times D$ matrix \mathbf{Y} , where the entry in row $n \in \{0, 1, \dots, N-1\}$ and column $k \in \mathcal{D}$ is $y_k^{(n)}$. From the $N \times D$ matrix \mathbf{Y} we create the $N \times D$ matrix \mathbf{Z} by taking the FFT of the columns of \mathbf{Y} . The m th row of \mathbf{Z} (for $m \in \mathcal{M}$) corresponds to the candidate Doppler $\omega = 2\pi m/L$, while the d -th column (for $d \in \mathcal{D}$) is the candidate code phase. A block diagram of core DEES can be adapted from Fig. 1, where \mathbf{Z} is produced directly from an FFT of the columns of \mathbf{Y} and where \mathbf{Y}_t , \mathbf{Z}_t and the series of Γ matrices can be ignored.

The maximum normalized Doppler frequency tested by the FFT is $2\pi(N/2 - 1)/L$. To prevent aliasing we must have $N > \omega_{\max}L/\pi + 2$, where $\omega_{\max} = 2\pi f_c T_c b_{0,\max}$ is the maximum normalized radian Doppler frequency. This places a lower bound on the number of segments needed. On the other hand, the DFT resolution, with no zero-padding, is given by $\Delta f = 1/(LT_c)$.

We now discuss how estimates of $\{d_0, b_0\}$ can be

obtained from \mathbf{Z} . Since DSSS signals have, ideally, thumbtack autocorrelation characteristics, one strategy to produce estimates is to search for distinct peaks in $|\mathbf{Z}|$. The code phase offset and Doppler frequency can be jointly estimated with row index $m \in \mathcal{M}$ and column index $k \in \mathcal{D}$, namely $\hat{b}_0 = m/(Lf_c T_c)$ and $\hat{d}_0 = k$. A non-unity α does not affect the estimation process of $\{d_0, b_0\}$.

It is important to note that the only difference between core DEES and an exhaustive search is the constant phase approximation. Thus as long as CPA holds, core DEES will produce the same estimates as the exhaustive search.

IV. TIME-VARYING CODE PHASES

We now relax the static code phase assumption and consider the received signal model in (1). Since d_k is a function of k , the code phase offset will shift over time as core DEES performs its partitioned matched filtering. Furthermore, the non-negligible Doppler rate will cause the Doppler frequency to change over time as well. The combination of both of these effects, sometimes referred to as code phase migration (CPM) and Doppler frequency migration (DFM) [29], respectively, will prevent coherent integration from (11), resulting in indistinct peaks in $|\mathbf{Z}|$, and greatly reducing acquisition performance. An example of this can be seen in the upper two panels of Fig. 2, where Fig. 2(a) depicts $|\mathbf{Y}|$ in the segment-code phase plane, where CPM for a two path channel is present. Since the FFT applied to \mathbf{Y} can only capture signal energy in a given column, the post-integration SNR is significantly reduced. Fig. 2(b) depicts $|\mathbf{Z}|$ in the code phase-Doppler plane, after the FFT of the columns of \mathbf{Y} . The two jagged lines indicate DFM is present for both channel paths.

Rather than redevelop DEES from an even more expensive exhaustive 3D search over parameters $\{d_0, b_0, b_1\}$, we instead choose to estimate and compensate for the Doppler rate, mitigate the effects of CPM and DFM, and finally acquire the quasi-static signal. This approach will adjust the problem from a 3D search to a 2D one, where core DEES is already derived from the optimal exhaustive search.

Our approach is to utilize a second-order keystone transform (SOKT) [25], [30] to mitigate the quadratic component of CPM, then use a fractional Fourier transform (FrFT) to estimate the Doppler rate, compensate for it with a complex phase factor, and finally apply another SOKT to remove any residual CPM and DFM. We first discuss each step in the ideal case in which digitization is a non-issue, then discuss a practical implementation of this approach.

Ignoring the noise component, the output of the n th MF is:

$$\begin{aligned} y_k^{(n)} &= r_k^{(n)} * x_{-k}^{*(n)} \\ &\approx \alpha x_{k-d_{nL/N}}^{(n)} e^{-j\omega_0 d_{nL/N}} * x_{-k}^{*(n)}, \end{aligned} \quad (12)$$

where in the last line it was assumed that since CPA holds such the delays within a given signal segment will not change, i.e. $d_{k+nL/N} \approx d_{nL/N}$.

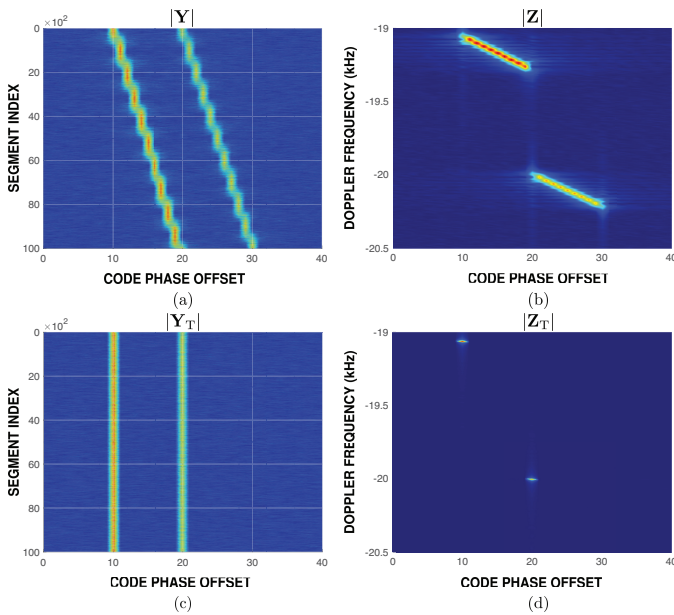


Fig. 2: Top-down view of $|Y|$ in (a) and $|Z|$ in (b) for core DEES, where both CPM and DFM is present. Once augmented with the SOKT and FrFT, DEES is able to remove the effects of both CPM and DFM, as seen in (c) and (d). Two path channel with $d_0 = \{10, 20\}$, $f_{D,0} = \{-19.1, -20.0\}$ kHz, and $f_A = \{-1.3, -1.3\}$ kHz/s. SNR = -10 dB, $L/N = 1000$.

Taking the DTFT of (12) with respect to k and expanding $d_{nL/N}$ yields:

$$Y(n, \omega') = \alpha X(n, \omega') X^*(n, \omega') e^{-j(\omega_0 + \omega') d_0} e^{j(\omega_0 + \omega')(b_0 n L/N + b_1 (n L/N)^2)}, \quad (13)$$

where ω' is the radian Fourier frequency and $X(n, \omega')$ is the DTFT of $x_k^{(n)}$. The $\exp(j\omega' b_0 n L/N)$ term in (13) is responsible for the linear component of CPM, while the $\exp(j\omega' b_1 (n L/N)^2)$ term is responsible for both the quadratic component of CPM and DFM.

First proposed in the context of synthetic aperture radar, the keystone transform (KT) is able to correct for linear time-varying delays without a priori knowledge of the target's Doppler frequency [31]. The KT has since been extended to a “second-order” form which can blindly correct for quadratic time-varying delays. The SOKT is [25], [30]:

$$n = \sqrt{\frac{\omega_0}{\omega_0 + \omega'}} n' \quad (14)$$

where n' is the transformed index. Substituting (14) into (13) yields:

$$Y(n', \omega') = \alpha X(n', \omega') X^*(n', \omega') e^{-j(\omega_0 + \omega') d_0} e^{j b_0 n' L/N \sqrt{\omega_0 (\omega_0 + \omega')}} e^{j \omega_0 b_1 (n' L/N)^2}, \quad (15)$$

where $X(n', \omega')$ is $X(n, \omega')$ after applying the SOKT. The $\exp(j b_0 n' L/N \sqrt{\omega_0 (\omega_0 + \omega')})$ term in (15) indicates a component of CPM still remains. However, this component

cannot be rectified with another SOKT due to the presence of the $\exp(j\omega_0 b_1 (n' L/N)^2)$ term. We instead use a FrFT to generate \hat{b}_1 , an estimate of b_1 , and then multiply (15) by $\exp(-j\omega_0 \hat{b}_1 (n' L/N)^2)$ to remove the nuisance term.

The FrFT can be used to estimate the chirp rate of an LFM signal [19], [24], [32], [33]. The continuous time FrFT of signal $x(t)$ is [33], [34]:

$$X(\beta, u) = \int_{-\infty}^{\infty} x(t) K_\beta(t, u) dt, \quad (16)$$

where β is the rotation angle, and $K_\beta(t, u)$ is:

$$K_\beta(t, u) = \begin{cases} \sqrt{1 - j \cot(\beta)} e^{j \pi \phi(t, u, \beta)} & \beta \neq n \\ \delta(t - u) & \beta \in 2n\pi \\ \delta(t + u) & \beta \in (2n \pm 1)\pi \end{cases}, \quad (17)$$

where $\phi(t, u, \beta) = t^2 \cot(\beta) + u^2 \cot(\beta) - tu \csc(\beta)$, and $n \in \mathbb{Z}$. The FrFT is equivalent to the canonical Fourier transform when $\beta = \pi/2$ [33], [34].

If $x(t)$ is an LFM signal of the form $A e^{j\pi(\mu t^2 + 2f_0 t + \phi_0)}$, then an estimate of its chirp rate $\hat{\mu}$ can be obtained from [24]:

$$\hat{\mu} = -\cot(\hat{\beta}), \quad (18)$$

where

$$\hat{\beta} = \arg \max_{\beta} |X(\beta, u)|^2. \quad (19)$$

When $x(t)$ is an LFM signal, then $|X(\beta, u)|^2$ will have thumbtack-like characteristics and $\hat{\beta}$ can be found via numerical search [33].

(15) can be approximated as an LFM signal with respect to n' with equivalent chirp rate $2b_1 f_c$, if the amplitude is constant. This condition will be satisfied when the segment size L/N is sufficiently large such that $X(n', \omega') X^*(n', \omega')$ is approximately constant. The quadratic coefficient, b_1 , can then be estimated in a similar fashion as (18).

If the estimates are accurate enough such that $\hat{b}_1 \approx b_1$, then multiplying (15) by $\exp(-j\omega_0 \hat{b}_1 (n' L/N)^2)$ and taking another SOKT yields:

$$Y(n'', \omega') = \alpha X(n'', \omega') X^*(n'', \omega') e^{-j(\omega_0 + \omega') d_0} e^{j \omega_0 b_0 n'' L/N}, \quad (20)$$

where n'' is the post SOKT index. From (20) it is apparent that there is no longer any coupling between ω' and n'' , which indicates that the effects of both CPM and DFM have been removed. This can be seen in the lower panels of Fig. 2, where the energy in $|Z_T|$ has been focused into two distinct peaks. The SOKTs remove the time-varying aspect of both the code phase and the Doppler shift, and fixes them at an arbitrary point; we chose the initial code phase and initial Doppler to allow for easy estimation of $\{d_0, b_0\}$.

We now discuss a practical implementation of these DEES augmentations. If an FFT of the rows of $N \times D$ matrix \mathbf{Y} are taken to produce matrix Γ , then the SOKT can be applied to the columns of Γ with sinc interpolation [35]:

$$\Gamma'_{n',l} = \sum_{n=0}^{N-1} \Gamma_{n,l} \text{sinc} \left[\sqrt{\frac{\omega_0}{\omega_0 + \frac{2\pi l}{D}}} n' - n \right], \quad (21)$$

to produce matrix Γ' , where Γ_{nl} refer to the n th row and l th column of Γ .

A discrete FrFT is then applied to each of the columns of Γ' , to obtain estimates of the equivalent chirp rates $\hat{\eta}_l = -\cot(\hat{\beta}_l)N/(T_c L)^2$, where $\hat{\beta}_l$ is the optimal FrFT angle of the l th column and $N/(T_c L)^2$ is a sampling correction factor for the discrete FrFT [36]. In principle, $\hat{\eta}_l = \hat{\eta} = 2b_1 f_c / T_c \forall l$, however, in practice it is necessary to average over all possible values. Namely:

$$\hat{b}_1 = \frac{T_c}{2f_c D} \sum_{l=0}^{D-1} \hat{\eta}_l. \quad (22)$$

The accuracy of \hat{b}_1 can further be improved at low SNR by removing extraneous values of $\hat{\eta}_l$, corresponding to \hat{b}_1 exceeding $b_{1,\max}$, before taking the mean.

The columns of Γ' are then multiplied by complex phase factor $\exp(-j\hat{b}_1 \pi (n' T_c L / N)^2)$, resulting in matrix Γ'' . An SOKT is applied to the columns of Γ'' in a similar fashion as (21), and finally an IFFT is applied to the rows of the resulting matrix to obtain $N \times D$ matrix \mathbf{Y}_T . A block diagram of the augmented DEES is shown in Fig. 1, where an FFT of the columns of \mathbf{Y}_T is taken in accordance with the core DEES algorithm.

V. NUMERICAL RESULTS

To demonstrate the efficacy of DEES, we characterize its acquisition performance in the LEO satellite channel as a function of SNR, and showcase its performance improvement over the core DEES algorithm.

We measure performance as probability of acquisition P_A for a fixed false alarm rate P_{FA} . P_A and P_{FA} are calculated by the fraction of trials that the decision statistic (3) exceeds threshold ζ when the signal component of r_k is present and absent, respectively. We assume that inaccurate estimates of $\{d_0, b_0, b_1\}$ will result in a negligible correlation.

For each SNR we simulate 1000 trials, where each trial has both independent noise and parameter realizations. Each parameter is drawn from a uniform distribution ranging from \pm its maximum value; for example d_0 is drawn from $\mathcal{U}(-d_{0,\max}, d_{0,\max})$. The polarity of b_0 and b_1 is enforced to be the same. The phase of α is uniformly distributed, and $|\alpha|$ is drawn from $\mathcal{U}(1, 5)$.

We consider a system with $f_c = 20$ GHz, $f_s = 1/T_c = 60$ MHz, $L = 2^{20}$, and $L/N = 500$ chips. For the LEO satellite channel, we consider the high acceleration regime [1], and select $d_{0,\max} = 20$, $b_{0,\max} = 2.0 \times 10^{-6}$, $b_{1,\max} = 2.36 \times 10^{-15}$, which with the previous system parameters corresponds to a maximum initial Doppler frequency shift of $f_{D,0} = 40$ kHz, a maximum Doppler rate of 5.67 kHz/s, a maximum of 2.10 code phase bins migrated, and a maximum of 1.73 Doppler bins migrated.

Shown in Fig. 3(a) is P_A vs. SNR (dB) for fixed $P_{FA} = 0.01$ for both DEES (purple curve) and core DEES (dark red curve). As the SNR increases, P_A also increases, with DEES achieving $P_A > 0.9$ when $\text{SNR} \geq -41$ dB. Once the SNR exceeds -40 dB, P_A has diminishing performance gains with

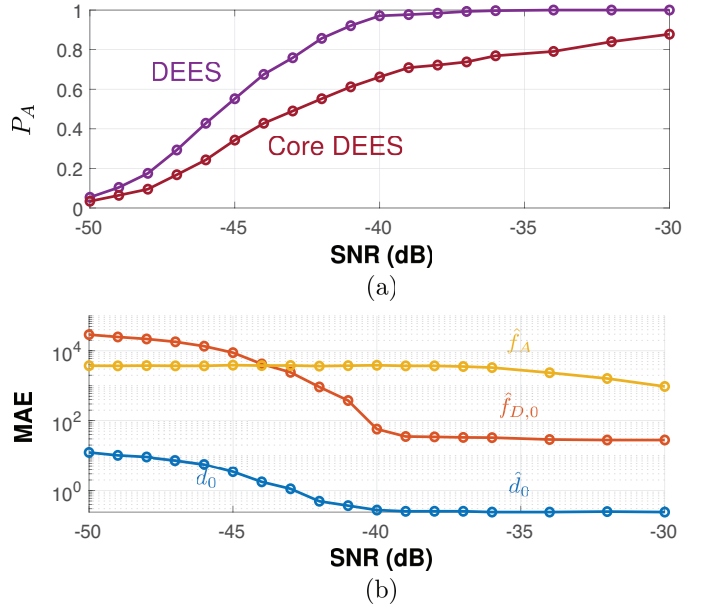


Fig. 3: (a) P_A vs. SNR (dB) for fixed $P_{FA} = 0.01$. (b) DEES Mean absolute error (MAE) vs. SNR (dB) for \hat{d}_0 (blue curve), $\hat{f}_{D,0}$ (red curve), and \hat{f}_A (gold curve).

increasing SNR, as \hat{d}_0 is now within a fraction of a chip of the true value, and the initial Doppler frequency estimate is now accurate to within tens of Hz. This can be seen in Fig. 3(b) which plots the mean absolute error (MAE) for $\{\hat{d}_0, \hat{f}_{D,0}, \hat{f}_A\}$ vs. SNR (dB) for DEES. DEES has difficulty obtaining an accurate \hat{f}_A when the SNR is low, as evidenced by the MAE obtaining an upper bound, which exists only due to knowledge of $b_{1,\max}$. However, when $\text{SNR} \geq -30$ dB, the Doppler rate error is less than 1 kHz/s, which is well within the pull-in range of tracking loops [37].

Due to the presence of both CPM and DFM, DEES outperforms core DEES by a wide margin. This can be seen in Fig. 3(a), where core DEES requires approximately 5 dB of additional SNR to achieve the same $P_A \approx 0.7$. The performance benefit of the DEES augmentations are more apparent as SNR increases, as evidenced by the widening gap between the purple and dark red curves.

VI. CONCLUSION

In this work we have proposed DEES, an algorithm that can acquire a long-code DSSS signal in the presence of both large Doppler shifts and high Doppler rate. DEES utilizes a composition of the SOKT and the FrFT to reduce an expensive 3D search into a 2D search with limited post-processing. Numerical results show DEES can acquire long-code DSSS signal in the high-acceleration regime of the LEO satellite channel, achieving greater than 90% acquisition rate with a 1% false alarm rate at SNRs as low as -41 dB.

REFERENCES

- [1] I. Ali, N. Al-Dhahir, and J. Hershey, "Doppler characterization for LEO satellites," *IEEE Transactions on Communications*,

- vol. 46, no. 3, pp. 309–313, Mar. 1998. [Online]. Available: <https://doi.org/10.1109/26.662636>
- [2] M. Lucente, T. Rossi, A. Jebril, M. Ruggieri, S. Pulitano, A. Iera, A. Molinaro, C. Sacchi, and L. Zuliani, “Experimental missions in W-band: A small leo satellite approach,” *IEEE Systems Journal*, vol. 2, no. 1, pp. 90–103, Mar. 2008. [Online]. Available: <https://doi.org/10.1109/jsyst.2007.914787>
- [3] T. Pratt, *Satellite communications*. Hoboken, NJ, USA: Wiley, 2020.
- [4] X. Ying and Y. Hong, “High-sensitivity acquisition of ultrahigh dynamic direct sequence spread spectrum signals in space communications,” *China Communications*, vol. 10, no. 10, pp. 26–36, Oct. 2013. [Online]. Available: <https://doi.org/10.1109/cc.2013.6650317>
- [5] Z. Zhang, W. Cheng, and H. Zhang, “Search-range-correction-based Doppler shift acquisition for space communications,” *IEEE Transactions on Vehicular Technology*, vol. 65, no. 5, pp. 3271–3284, May 2016. [Online]. Available: <https://doi.org/10.1109/tvt.2015.2432456>
- [6] L. Shi, L. Zhao, C. Zhang, and B. Yao, “Fast telemetry and communication scheme based on doppler diversity reception under large dynamic doppler for hypersonic vehicles,” *Electronics*, vol. 8, no. 7, 2019. [Online]. Available: <https://www.mdpi.com/2079-9292/8/7/781>
- [7] D. Torrieri, *Principles of Spread-Spectrum Communication Systems*, 3rd ed. Springer Publishing Company, Incorporated, 2015.
- [8] L. Simone, G. Fittipaldi, and I. A. Sanchez, “Fast acquisition techniques for very long PN codes for on-board secure TTC transponders,” in *2011 - MILCOM 2011 Military Communications Conference*. IEEE, Nov. 2011. [Online]. Available: <https://doi.org/10.1109/milcom.2011.6127563>
- [9] S. M. Spangenberg, I. Scott, S. McLaughlin, G. J. Povey, D. G. Cruickshank, and P. M. Grant, “An FFT-based approach for fast acquisition in spread spectrum communication systems,” *Wireless Personal Communications*, vol. 13, no. 1, pp. 27–55, May 2000. [Online]. Available: <https://doi.org/10.1023/A:1008848916834>
- [10] R. A. Stirling-Gallacher, A. P. Hulbert, and G. J. R. Povey, “A fast acquisition technique for a direct sequence spread spectrum signal in the presence of a large Doppler shift,” in *Proceedings of ISSSTA'95 International Symposium on Spread Spectrum Techniques and Applications*, vol. 1, Sep. 1996, pp. 156–160 vol.1.
- [11] H. Saarnisaari and E. Karami, “Frequency domain block filtering GNSS receivers,” in *2008 IEEE/ION Position, Location and Navigation Symposium*, May 2008, pp. 159–166.
- [12] E. Karami and H. Saarnisaari, “Windowed overlapped frequency domain block filtering approach for direct sequence signal acquisition,” *Digital Communications and Networks*, vol. 4, no. 3, pp. 209–216, Aug. 2018. [Online]. Available: <https://doi.org/10.1016/j.dcan.2017.04.006>
- [13] N. Ziedan and J. Garrison, “Unaided acquisition of weak GPS signals using circular correlation or double-block zero padding,” in *PLANS 2004. Position Location and Navigation Symposium (IEEE Cat. No.04CH37556)*. IEEE. [Online]. Available: <https://doi.org/10.1109/plans.2004.1309030>
- [14] M. Foucras, O. Julien, C. Macabiau, and B. Ekambi, “A novel computationally efficient Galileo E1 OS acquisition method for GNSS software receiver,” in *ION GNSS 2012, 25th International Technical Meeting of The Satellite Division of the Institute of Navigation*, Nashville, United States, Sep. 2012, p. pp xxxx. [Online]. Available: <https://hal-enac.archives-ouvertes.fr/hal-00938830>
- [15] G. E. Corazza and R. Pedone, “Generalized and average likelihood ratio testing for post detection integration,” *IEEE Transactions on Communications*, vol. 55, no. 11, pp. 2159–2171, Nov. 2007. [Online]. Available: <https://doi.org/10.1109/tcomm.2007.908531>
- [16] N. Ziedan, *GNSS receivers for weak signals*. Norwood, MA: Artech House, 2006.
- [17] H. Luo, Y. Wang, Z. Ma, and S. Wu, “A segmentation motion compensation-based longterm integration method for DSSS signal,” in *2012 IEEE 11th International Conference on Signal Processing*. IEEE, Oct. 2012. [Online]. Available: <https://doi.org/10.1109/icosp.2012.6491811>
- [18] Z. Sun, X. Li, W. Yi, G. Cui, and L. Kong, “Range walk correction and velocity estimation for high-speed target detection,” in *2017 IEEE Radar Conference (RadarConf)*. IEEE, May 2017. [Online]. Available: <https://doi.org/10.1109/radar.2017.7944440>
- [19] Y. Luo, L. Zhang, and H. Ruan, “An acquisition algorithm based on FRFT for weak GNSS signals in a dynamic environment,” *IEEE Communications Letters*, vol. 22, no. 6, pp. 1212–1215, Jun. 2018. [Online]. Available: <https://doi.org/10.1109/lcomm.2018.2828834>
- [20] Y. Luo, C. Yu, S. Chen, J. Li, H. Ruan, and N. El-Sheimy, “A novel Doppler rate estimator based on fractional Fourier transform for high-dynamic GNSS signal,” *IEEE Access*, vol. 7, pp. 29 575–29 596, 2019. [Online]. Available: <https://doi.org/10.1109/access.2019.2903185>
- [21] S. Wu, J. Tian, and W. Cui, “A novel parameter estimation algorithm for DSSS signals based on compressed sensing,” *Chinese Journal of Electronics*, vol. 24, no. 2, pp. 434–438, Apr. 2015. [Online]. Available: <https://doi.org/10.1049/cje.2015.04.035>
- [22] X. Li, Z. Sun, W. Yi, G. Cui, and L. Kong, “Radar detection and parameter estimation of high-speed target based on MART-LVT,” *IEEE Sensors Journal*, vol. 19, no. 4, pp. 1478–1486, Feb. 2019. [Online]. Available: <https://doi.org/10.1109/jsen.2018.2882198>
- [23] X. Li, G. Cui, W. Yi, and L. Kong, “Fast coherent integration for maneuvering target with high-order range migration via TRT-SKT-LVD,” *IEEE Transactions on Aerospace and Electronic Systems*, vol. 52, no. 6, pp. 2803–2814, Dec. 2016. [Online]. Available: <https://doi.org/10.1109/taes.2016.150573>
- [24] J. Tian, W. Cui, and S. Wu, “A novel method for parameter estimation of space moving targets,” *IEEE Geoscience and Remote Sensing Letters*, vol. 11, no. 2, pp. 389–393, Feb. 2014. [Online]. Available: <https://doi.org/10.1109/lgrs.2013.2263332>
- [25] X. Li, G. Cui, W. Yi, L. Kong, and J. Yang, “Range migration correction for maneuvering target based on generalized keystone transform,” in *2015 IEEE Radar Conference (RadarCon)*. IEEE, May 2015. [Online]. Available: <https://doi.org/10.1109/radar.2015.7130977>
- [26] C. O’Driscoll, “Performance analysis of the parallel acquisition of weak GPS signals,” Ph.D. dissertation, University College Cork, 2007.
- [27] W. Hurd, J. Statman, and V. Vilnrotter, “High dynamic GPS receiver using maximum likelihood estimationand frequency tracking,” *IEEE Transactions on Aerospace and Electronic Systems*, vol. AES-23, no. 4, pp. 425–437, Jul. 1987. [Online]. Available: <https://doi.org/10.1109/taes.1987.310876>
- [28] H. L. V. Trees, *Detection, Estimation, and Modulation Theory: Radar-Sonar Signal Processing and Gaussian Signals in Noise*. Melbourne, FL, USA: Krieger Publishing Co., Inc., 1992.
- [29] Y. Shen and Y. Xu, “Analysis of the code phase migration and Doppler frequency migration effects in the coherent integration of direct-sequence spread-spectrum signals,” *IEEE Access*, vol. 7, pp. 26 581–26 594, 2019. [Online]. Available: <https://doi.org/10.1109/access.2019.2900279>
- [30] K. M. Scott, W. C. Barott, and B. Himed, “The keystone transform: Practical limits and extension to second order corrections,” in *2015 IEEE Radar Conference (RadarCon)*. IEEE, May 2015. [Online]. Available: <https://doi.org/10.1109/radar.2015.7131189>
- [31] R. P. Perry, R. C. DiPietro, and R. L. Fante, “SAR imaging of moving targets,” *IEEE Transactions on Aerospace and Electronic Systems*, vol. 35, no. 1, pp. 188–200, Jan 1999.
- [32] H.-B. Sun, G.-S. Liu, H. Gu, and W.-M. Su, “Application of the fractional Fourier transform to moving target detection in airborne SAR,” *IEEE Transactions on Aerospace and Electronic Systems*, vol. 38, no. 4, pp. 1416–1424, Oct. 2002. [Online]. Available: <https://doi.org/10.1109/taes.2002.1145767>
- [33] A. Serbes and O. Aldimashki, “A fast and accurate chirp rate estimation algorithm based on the fractional Fourier transform,” in *2017 25th European Signal Processing Conference (EUSIPCO)*. IEEE, Aug. 2017. [Online]. Available: <https://doi.org/10.23919/eusipco.2017.8081379>
- [34] L. Almeida, “The fractional Fourier transform and time-frequency representations,” *IEEE Transactions on Signal Processing*, vol. 42, no. 11, pp. 3084–3091, 1994. [Online]. Available: <https://doi.org/10.1109/78.330368>
- [35] T. Deng and C. Jiang, “Evaluations of keystone transforms using several interpolation methods,” in *Proceedings of 2011 IEEE CIE International Conference on Radar*, vol. 2, Oct 2011, pp. 1876–1878.
- [36] B. Deng, J. bao Luan, and S. qi Cui, “Analysis of parameter estimation using the sampling-type algorithm of discrete fractional Fourier transform,” *Defence Technology*, vol. 10, no. 4, pp. 321–327, Dec. 2014. [Online]. Available: <https://doi.org/10.1016/j.dt.2014.06.011>
- [37] Y. Guo, H. Huan, R. Tao, and Y. Wang, “Frequency tracking loop with wide pull-in range for weak DSSS signal,” *Electronics Letters*, vol. 54, no. 23, pp. 1336–1338, Nov. 2018. [Online]. Available: <https://doi.org/10.1049/el.2018.6631>